

## Correlated-effective-field treatment of the anisotropic Ising ferromagnet: Thermodynamical properties

R. Honmura

*Departamento de Física, Universidade Federal de Alagoas 57000, Maceió, Al-Brazil*

*and Department of Physics, Nagoya University, Nagoya 464, Japan*

(Received 26 October 1983)

Within a new type of correlated-effective-field theory we calculate the effective-field parameters (including their response to external field), critical temperatures, susceptibility, short-range order parameters, and specific heat associated with an anisotropic, square-lattice, spin- $\frac{1}{2}$  Ising ferromagnet. The present formalism, which is shown to recover the Bethe-Peierls thermodynamics for the pure Z-coordinated-lattice, spin- $\frac{1}{2}$  Ising model, yields satisfactory results; in particular, the crossover from a pure Ising ferromagnet on a square lattice to that on a linear chain is reasonably exhibited in the behavior of the susceptibility and the specific heat.

### I. INTRODUCTION

The Ising model has been one of the most actively studied problems in statistical mechanics. Rigorous solutions have been given for the simple model for one-dimensional and certain two-dimensional lattices.<sup>1</sup> In three-dimensional lattices there are series-expansion methods,<sup>2</sup> which are valid for temperatures either high or low compared with the critical temperature, as well as renormalization-group methods.<sup>3</sup>

On the other hand, the molecular-field approximation (MFA), because of its simplicity, has played an important role in the description of cooperative phenomena. The MFA gives qualitative agreement with experiments for many of the physical quantities involved in a phase transition. However, the MFA has some deficiencies, which are due to the neglect of correlations when MFA results are compared with experiments. These deficiencies become so serious when the system studied is complex that the MFA may not predict important features characteristic of such a complex system. Improvements in this respect have been sought in many methods.<sup>4</sup>

Recently, Lines<sup>5</sup> has suggested that static correlations can be partially accounted for by the introduction of an extra term in the effective field "experienced" by spin  $S_i$ . This term is proportional to the instantaneous deviation of  $S_i$  from its average value. The constant of this proportionality, called the correlated effective-field parameter, is determined by imposing consistency on the theory with an exact sum rule for the susceptibility at the end of the calculation. The correlated effective-field approximation (CEFA) developed by Lines has been applied to a number of problems in magnetic systems.<sup>6</sup> However, this method gives an accuracy essentially equivalent to that of the spherical model, and unfortunately the sum rule is only valid often in the paramagnetic phase<sup>7</sup> and in the absence of the resulting strong, induced anisotropic fields. Moreover, when the CEFA is applied to the two-dimensional ferromagnetic Ising lattice, the theory generally predicts vanishing critical temperatures.<sup>8</sup>

Very recently, Kaneyoshi *et al.*<sup>9</sup> developed a new type of correlated effective-field theory for the spin- $\frac{1}{2}$  pure Ising model on a regular lattice. This theory is based on incorporating the concept of a correlated effective field into the exact formal identities, the so-called Callen identities,<sup>10</sup> to which the exponential-operator technique introduced by Honmura and Kaneyoshi<sup>11</sup> is utilized. Contrary to the CEFA, this new type of theory does not use an effective-field Hamiltonian. The resulting statistical theory is shown to give critical temperatures equivalent to that of the Bethe-Peierls (BP) method and should be compared with the CEFA. This statistical theory has already been applied to a variety of interesting situations such as pure anisotropic systems,<sup>12</sup> dilute ferromagnets,<sup>13,14</sup> and surface ferromagnets.<sup>15</sup> Most of these works have been devoted to the analysis of the phase diagram and spontaneous magnetization of those systems.

In the present work we study the anisotropic square-lattice spin- $\frac{1}{2}$  Ising ferromagnet. The relevant thermodynamical quantities, namely the correlated effective-field parameters including their response in a vanishingly small external field, the phase diagram, the spontaneous magnetization, the short-range order parameter, the specific heat, and the susceptibility, are all calculated within a new type of correlated effective-field theory (NCEFT). The present work, the formalism of which has only small differences from that of Refs. 9 and 12, yields analytical solutions for all of the above-mentioned thermodynamical properties. Although, of course, we do not expect the NCEFT to yield accurate values in the critical region due to the absence of long-range fluctuations, we do expect reasonable values for the plot of critical temperature versus anisotropic parameter, and also for the specific heat and susceptibility. In particular, since the NCEFT reduces to the exact solution in the one-dimensional lattice, the cross-over phenomena from the two-dimensional to the one-dimensional case is clearly exhibited in the behavior of the specific heat and the susceptibility.

In the next section we briefly review the formalism of the NCEFT. In Sec. III the theory is applied to the aniso-

tropic square-lattice spin- $\frac{1}{2}$  Ising ferromagnet. The analytical solutions of the most relevant thermodynamical quantities are also obtained in Sec. III. In Sec. IV the numerical results of such quantities are shown. In Sec. V we show that the theory is essentially equivalent to BP method for pure Ising ferromagnets on a  $Z$ -coordinated lattice.

## II. FORMALISM: A NEW TYPE OF CORRELATED EFFECTIVE-FIELD THEORY

Recently, in Ref. 9, we have introduced a new type of correlated effective-field theory (NCEFT) for the Ising model. In this section we shall briefly review this approximation for the pure Ising ferromagnet for the sake of completeness.

The Hamiltonian for the spin- $\frac{1}{2}$  ( $\hbar=1$ ) Ising ferromagnet in an external magnetic field  $H$  is given by

$$\mathcal{H} = - \sum_{\langle i,j \rangle} J_{ij} \sigma_i \sigma_j - g \mu_B H \sum_j \sigma_j, \quad \sigma_j = \pm 1 \quad (1)$$

where  $\langle i,j \rangle$  runs over all nearest-neighbor (NN) spins,  $J_{ij}$  is the exchange interaction between NN spins,  $g$  is the Landé factor, and  $\mu_B$  is the Bohr magneton.

Formal identities for the correlation functions of the Ising model have appeared in previous literature.<sup>16</sup> The starting point here for the statistics of our spin system is the exact Callen<sup>10</sup> equation

$$\langle \sigma_i \bar{f}_i \rangle = \left\langle \bar{f}_i \tanh \left[ \sum_j \beta J_{ij} \sigma_j + h \right] \right\rangle, \quad (2)$$

where the angular brackets designate the usual ensemble average

$$\langle \cdots \rangle = \text{Tr}[\exp(-\beta \mathcal{H}) \cdots] / \text{Tr}[\exp(-\beta \mathcal{H})],$$

where  $\beta = (k_B T)^{-1}$ ,  $h = \beta g \mu_B H$ , and  $\bar{f}_i$  represents any function of the Ising variables except  $\sigma_i$ . Following Ref. 11 we now introduce the differential operator  $D \equiv \partial / \partial x$  into Eq. (2) and obtain

$$\begin{aligned} \langle \sigma_i \bar{f}_i \rangle &= \left\langle \bar{f}_i \exp \left[ \sum_j D \beta J_{ij} \sigma_j \right] \right\rangle \tanh(x+h) \Big|_{x=0} \\ &= \left\langle \bar{f}_i \prod_{j=1}^Z [\cosh(D \beta J_{ij}) \right. \\ &\quad \left. + \sigma_j \sinh(D \beta J_{ij})] \right\rangle \tanh(x+h) \Big|_{x=0}, \end{aligned} \quad (3)$$

where  $Z$  is the coordination number. Since we are interested in the thermodynamical quantities, let us expand the right-hand side (rhs) of the above equation with respect to  $h$  and retain only its first-order terms,

$$\langle \sigma_i \bar{f}_i \rangle = \langle \bar{f}_i \hat{K} \rangle + \langle \bar{f}_i \hat{G} \rangle h, \quad (4)$$

where

$$\hat{K} = \prod_{j=1}^Z [\cosh(D \beta J_{ij}) + \sigma_j \sinh(D \beta J_{ij})] \tanh x \Big|_{x=0}, \quad (5a)$$

$$\hat{G} = \prod_{j=1}^Z [\cosh(D \beta J_{ij}) + \sigma_j \sinh(D \beta J_{ij})] \text{sech}^2 x \Big|_{x=0}. \quad (5b)$$

Equation (4) can generate many kinds of identities, which give relations among spin correlation functions, upon substituting some Ising variable functions for  $\bar{f}_i$ . Among them, upon setting  $\bar{f}_i = 1$ , Eq. (4) reduces to

$$\langle \sigma_i \rangle = \langle \hat{K} \rangle + \langle \hat{G} \rangle h, \quad (6)$$

which expresses the single-site magnetization in terms of multisite correlation functions which are yet undetermined. However, it is clear that if we try to treat exactly all the spin correlations present in (6), the problem becomes mathematically untractable.

In order to evaluate Eq. (6) many authors<sup>11,17</sup> have introduced an approximation which decouples next-neighbor spin correlations,

$$\langle \sigma_{j_1} \sigma_{j_2} \cdots \sigma_{j_Z} \rangle \simeq \langle \sigma_{j_1} \rangle \langle \sigma_{j_2} \rangle \cdots \langle \sigma_{j_Z} \rangle, \quad (7)$$

where  $j_1, j_2, \dots, j_Z$  are the NN's of site  $i$ . This approximation, called the effective-field approximation (EFA), yielded, in spite of its simplicity, quite satisfactory results in many interesting situations.<sup>18</sup> In particular, the EFA essentially corresponds to the Zernike<sup>19</sup> approximation for the regular lattice system.

On the other hand, Kaneyoshi *et al.*<sup>9</sup> (KFHM) have refined this approximation by introducing a NN correlated effective-field parameter  $\lambda$ . Following them, we assume that the NN Ising variables can be related to the central site  $i$  via

$$\sigma_{i+\delta} = \langle \sigma_{i+\delta} \rangle + \lambda_{i+\delta} (\sigma_i - \langle \sigma_i \rangle), \quad (8)$$

where  $\delta$  runs over the NN sites of the central site  $i$ , and  $\lambda_{i+\delta}$  is a temperature- and external-field-dependent correlated effective-field parameter.

Substitution of Eq. (8) into Eq. (6) gives an equation including the parameters  $m$ ,  $\beta J_{ij}$ ,  $\lambda_{i+\delta}$ , and  $h$ . Accordingly, in order to evaluate thermodynamical properties such as magnetization and critical temperature, we need an additional equation specifically for determining the parameters  $\lambda_{i+\delta}$  as a function of temperature.

In Ref. 9 we used a second identity

$$\langle \sigma_i \sigma_{i+\delta} \rangle = \langle \sigma_{i+\delta} \hat{K} \rangle + \langle \sigma_{i+\delta} \hat{G} \rangle h.$$

However, when we use higher-order correlation functions, such as the three-site identity

$$\langle \sigma_i \sigma_{i+\delta} \sigma_{i+\delta'} \rangle = \langle \sigma_{i+\delta} \sigma_{i+\delta'} \hat{K} \rangle + \langle \sigma_{i+\delta} \sigma_{i+\delta'} \hat{G} \rangle h,$$

we can easily prove that  $\lambda$  can be determined analytically. In the next section we shall clarify the importance of the higher-order correlation functions in order to obtain the analytical forms for the physical properties of the anisotropic square-lattice spin- $\frac{1}{2}$  Ising ferromagnets.

Finally, we should be careful in the selection of functions such as  $\bar{f}_i$  in Eq. (4). Recently, Taggart and Fittipaldi<sup>20</sup> have also applied the NCEFT to Ising systems. However, in order to determine the parameter  $\lambda$ , they introduced another identity which is obtained by simply setting  $\bar{f}_i = \coth(\beta \sum_j J_{ij} \sigma_j)$  in Eq. (4). From the beginning, for zero external field, their identity neglects the possible spin configurations resulting in  $\sum_j J_{ij} \sigma_j = 0$ , for which Eq. (4)

cannot be defined. Accordingly, it does not seem to be reasonable to use this function as  $\bar{f}_i$ .

### III. ANISOTROPIC SQUARE-LATTICE SPIN- $\frac{1}{2}$ ISING FERROMAGNET

In this section we study the thermodynamical properties of the square-lattice spin- $\frac{1}{2}$  Ising model with the anisotropic interactions  $J_1$  for the  $x$  direction and  $J_2$  for the  $y$  direction. Kaneyoshi and Tamura<sup>12</sup> (KT) studied this system on the basis of the NCEFT. Our aim in this paper is to rederive their results in an analytical form, although KT obtained them only numerically. Furthermore, the most relevant thermodynamical quantities, namely susceptibility and specific heat, are evaluated. In the course of analysis it is proved that the NCEFT becomes exact in the one-dimensional lattice limit.

We shall focus our attention on a system of  $S = \frac{1}{2}$  Ising spins arrayed on a square lattice interacting through the Hamiltonian (1), where  $J_{ij}$  takes  $J_1$  for NN spins in the  $x$  direction and  $J_2$  for NN spins in the  $y$  direction.

In the limit that the interaction ratio  $\alpha = J_2/J_1 \rightarrow 1$ , the model becomes a simple, spatially isotropic two-dimensional (2D) model, but as  $\alpha \rightarrow 0$  the system separates into a collection of noninteracting chains. Consequently, this system admits the crossover from the square lattice to the linear chain. Our starting point is Eqs. (4), (5a), and (5b) with  $Z=4$ , where  $\sigma_1$  and  $\sigma_3$  ( $\sigma_2$  and  $\sigma_4$ ) are the "right" and "left" ("up" and "down") NN spins of the site  $i$ .

At this point we develop the following three identities. By setting  $\bar{f}_i = 1$  in Eq. (4), we obtain

$$\begin{aligned} \langle \sigma_i \rangle &= 2(K_1 + K_2) \langle \sigma_1 \rangle + 2K_3 \langle \sigma_1 \sigma_2 \sigma_3 \rangle + 2K_4 \langle \sigma_1 \sigma_2 \sigma_4 \rangle \\ &+ h (G_1 + 4G_2 \langle \sigma_1 \sigma_2 \rangle + G_3 \langle \sigma_1 \sigma_3 \rangle \\ &+ G_4 \langle \sigma_2 \sigma_4 \rangle + G_5 \langle \sigma_1 \sigma_2 \sigma_3 \sigma_4 \rangle), \end{aligned} \quad (9)$$

by setting  $\bar{f}_i = \sigma_1 \sigma_3$ , we obtain

$$\begin{aligned} \langle \sigma_1 \sigma_1 \sigma_3 \rangle &= 2(K_1 + K_3) \langle \sigma_1 \rangle \\ &+ 2K_2 \langle \sigma_1 \sigma_2 \sigma_3 \rangle + 2K_4 \langle \sigma_1 \sigma_2 \sigma_4 \rangle \\ &+ h (G_1 \langle \sigma_1 \sigma_3 \rangle + 4G_2 \langle \sigma_1 \sigma_2 \rangle + G_3 \\ &+ G_4 \langle \sigma_1 \sigma_2 \sigma_3 \sigma_4 \rangle + G_5 \langle \sigma_2 \sigma_4 \rangle), \end{aligned} \quad (10)$$

and by setting  $\bar{f}_i = \sigma_2 \sigma_4$ , we obtain

$$\begin{aligned} \langle \sigma_i \sigma_2 \sigma_4 \rangle &= 2(K_2 + K_4) \langle \sigma_i \rangle \\ &+ 2K_1 \langle \sigma_1 \sigma_2 \sigma_4 \rangle + 2K_3 \langle \sigma_1 \sigma_3 \sigma_4 \rangle \\ &+ h (G_1 \langle \sigma_2 \sigma_4 \rangle + 4G_2 \langle \sigma_1 \sigma_2 \rangle \\ &+ G_3 \langle \sigma_1 \sigma_2 \sigma_3 \sigma_4 \rangle + G_4 + G_5 \langle \sigma_1 \sigma_3 \rangle), \end{aligned} \quad (11)$$

where obvious symmetrical relations  $\langle \sigma_1 \rangle = \langle \sigma_3 \rangle$ ,  $\langle \sigma_1 \sigma_2 \sigma_3 \rangle = \langle \sigma_1 \sigma_3 \sigma_4 \rangle$ , and  $\langle \sigma_1 \sigma_2 \rangle = \langle \sigma_2 \sigma_3 \rangle \neq \langle \sigma_1 \sigma_3 \rangle = \langle \sigma_2 \sigma_4 \rangle$  are used, and also where the coefficients  $K_i$  and  $G_i$  ( $i=1-5$ ) are given in the Appendix, where  $t$  denotes  $J_1/k_B T$ .

In order to obtain physical properties from the exact Eqs. (9)–(11), let us now introduce the concept of the correlated effective field into the multisite correlation functions of neighboring spins  $\sigma_1, \sigma_2, \sigma_3$ , and  $\sigma_4$ . Since we are dealing with an anisotropic 2D Ising model, our central assumption (8) can, of course, be changed into the following forms:

$$\sigma_{1,3} = \langle \sigma_{1,3} \rangle + \lambda_1 (\sigma_i - \langle \sigma_i \rangle), \quad (12)$$

$$\sigma_{2,4} = \langle \sigma_{2,4} \rangle + \lambda_2 (\sigma_i - \langle \sigma_i \rangle),$$

where the correlated effective-field parameters (CEFP's)  $\lambda_1$  and  $\lambda_2$  should be different from each other depending on the ratio  $\alpha$  and external field  $h$ .

Applying our approximation, Eq. (12), into multisite spin correlation functions appearing in Eqs. (9)–(11), we obtain

$$0 = (A_l - B_l m^2) m + h C_l, \quad l = 1, 2, 3 \quad (13)$$

where  $l=1$  is derived from Eq. (9),  $l=2$  from (10), and  $l=3$  from (11), and

$$A_l = \tanh[2t(1+\alpha)] - 1 + B_l, \quad l = 1, 2, 3 \quad (14)$$

$$B_1 = 2K_3 a + 2K_4 b, \quad (15)$$

$$B_2 = 2K_2 a + 2K_4 b + (1 - \lambda_1)^2, \quad (16)$$

$$B_3 = 2K_3 a + 2K_1 b + (1 - \lambda_2)^2 \quad (17)$$

$$a = (1 - \lambda_1)(2\lambda_1 \lambda_2 - \lambda_1 - 1), \quad (18)$$

$$b = (1 - \lambda_2)(2\lambda_1 \lambda_2 - \lambda_2 - 1), \quad (19)$$

with  $t \equiv \beta J_1$  and  $\alpha = J_2/J_1$ , and  $C_1$  is the coefficient for the  $h$  term on the rhs of Eq. (9),  $C_2$  for that on the rhs of Eq. (10), and  $C_3$  that on the rhs of Eq. (11), where the correlation functions appearing in these equations are now expressed as follows:

$$\langle \sigma_1 \sigma_2 \rangle = m^2 + (1 - m^2) \lambda_1 \lambda_2, \quad (20)$$

$$\langle \sigma_1 \sigma_3 \rangle = m^2 + (1 - m^2) \lambda_1^2, \quad (21)$$

$$\langle \sigma_2 \sigma_4 \rangle = m^2 + (1 - m^2) \lambda_2^2, \quad (22)$$

$$\begin{aligned} \langle \sigma_1 \sigma_2 \sigma_3 \sigma_4 \rangle &= m^4 + m^2 (1 - m^2) [\lambda_1^2 + \lambda_2^2 \\ &+ 4\lambda_1 \lambda_2 (1 - \lambda_1 - \lambda_2)] \\ &+ (1 - m^2) (1 + 3m^2) \lambda_1^2 \lambda_2^2. \end{aligned} \quad (23)$$

By using Eq. (13) with Eqs. (14)–(23), we can evaluate some thermodynamical properties of the anisotropic 2D Ising model.

#### A. Magnetization and correlated effective-field parameters

We turn to a study of the system with no external field,  $h=0$ . Equation (13) now admits two solutions, namely the paramagnetic ( $m=0$ ) and the nontrivial solutions (associated with the ferromagnetic phase) given by

$$m^2 = \frac{A_1}{B_1} = \frac{A_2}{B_2} = \frac{A_3}{B_3}, \quad (24)$$

from which we obtain the following coupled equations for the CEF's  $\lambda_1$  and  $\lambda_2$ :

$$(1 - \lambda_1) + 2(K_2 - K_3)(2\lambda_1\lambda_2 - \lambda_1 - 1) = 0, \quad (25a)$$

$$(1 - \lambda_2) + 2(K_1 - K_4)(2\lambda_1\lambda_2 - \lambda_2 - 1) = 0. \quad (25b)$$

We can easily solve these equations as follows:

$$\lambda_1 = \frac{e^{4t(1-\alpha)}}{e^{4t} - 1}, \quad T \leq T_c(\alpha) \quad (26)$$

$$m = \left[ 1 - \frac{4}{2 + 2 \cosh[4t(1-\alpha)] - 2[\exp(4t) + \exp(4t\alpha)] + \exp[4t(1+\alpha)]} \right]^{1/2}. \quad (28)$$

### B. Critical temperature

At the critical temperature  $T = T_c(\alpha)$ , the magnetization reduces to zero. Consequently, we have

$$1 = e^{-2t_c} + e^{-2t_c\alpha}, \quad (29)$$

where  $t_c = J_1/k_B T_c(\alpha)$ , which provides the critical temperature,

$$\frac{k_B T_c(\alpha)}{J_1} = \begin{cases} \frac{2}{\ln 2} \simeq 2.885 & \text{for } \alpha = 1, \\ 0 & \text{for } \alpha = 0. \end{cases} \quad (30)$$

The results (30) are simply those of the BP method.

### C. Susceptibility

The initial susceptibility is defined by

$$\chi = \lim_{H \rightarrow 0} \frac{\partial m}{\partial H} = \frac{(g\mu_B)^2}{k_B T} \frac{\partial m}{\partial h} \Big|_{h=0}. \quad (31)$$

Differentiating both sides of Eq. (13) (for  $l=1,2,3$ ) with  $h$ , we obtain

$$0 = (A_l - 3m^2 B_l) \frac{\partial m}{\partial h} + m(1 - m^2) \times \left[ \frac{\partial B_l}{\partial \lambda_1} \frac{\partial \lambda_1}{\partial h} + \frac{\partial B_l}{\partial \lambda_2} \frac{\partial \lambda_2}{\partial h} \right] + C_l, \quad l=1,2,3 \quad (32)$$

from which, upon using Eqs. (26)–(28), the initial susceptibility and response functions

$$\frac{\partial \lambda_1}{\partial h} \Big|_{h=0} \quad \text{and} \quad \frac{\partial \lambda_2}{\partial h} \Big|_{h=0}$$

below critical temperature can be calculated. In particular, as  $\alpha \rightarrow 1$  the inverse initial susceptibility reduces to

$$\left[ \frac{J_1}{(g\mu_B)^2} \chi \right]^{-1} = \frac{2(A_1 - FA_2)}{t(C_1 - FC_2)} \quad \text{for } \alpha = 1, \quad T \leq T_c(1), \quad (33)$$

$$\lambda_2 = \frac{e^{4t(\alpha-1)}}{e^{4t\alpha} - 1}, \quad T \leq T_c(\alpha). \quad (27)$$

It should be noted that expressions (26) and (27) are only valid below a critical temperature  $T_c(\alpha)$ , since in order to determine  $\lambda_1$  and  $\lambda_2$  we used the averaged magnetization equation (24). For temperatures above  $T_c(\alpha)$ , other equations for  $\lambda_1$  and  $\lambda_2$  will be obtained later [see Eqs. (36a) and (36b)].

Finally, magnetization is given, upon substituting (26) and (27) into (24), as a function of the temperature and interaction ratio  $\alpha$ ,

where

$$F = \frac{\tanh(4t) - 2 \tanh(2t)}{\tanh(4t) - \frac{2}{3}(e^{4t} - 1)}. \quad (34)$$

On the other hand, the inverse paramagnetic susceptibility is, through Eq. (32), given by

$$\left[ \frac{J_1}{(g\mu_B)^2} \chi_{\text{para}} \right]^{-1} = -\frac{A_1}{tC_1} = -\frac{A_2}{tC_2} = -\frac{A_3}{tC_3} \quad \text{for } T > T_c(\alpha). \quad (35)$$

By solving the coupled equations above, we can prove that the CEF's are given by

$$\lambda_1 = \tanh t \quad \text{for } T \geq T_c(\alpha), \quad (36a)$$

$$\lambda_2 = \tanh(\alpha t) \quad \text{for } T \geq T_c(\alpha). \quad (36b)$$

By using these solutions in Eq. (35), the inverse paramagnetic susceptibility can be evaluated. In particular, as  $\alpha \rightarrow 0$ , Eq. (35) reduces to

$$\left[ \frac{J_1}{(g\mu_B)^2} \chi_{\text{para}} \right]^{-1} = \frac{e^{-2t}}{t} \quad \text{for } \alpha = 0, \quad (37)$$

where this is simply the exact expression for the one-dimensional Ising model.

Finally, the response functions of CEF's in external field,

$$\frac{\partial \lambda_1}{\partial h} \Big|_{h=0} \quad \text{and} \quad \frac{\partial \lambda_2}{\partial h} \Big|_{h=0},$$

are obtained only for the region  $T \leq T_c(\alpha)$  by solving the coupled equations (32). In particular, as  $\alpha \rightarrow 1$  they reduce to

$$\begin{aligned} \frac{\partial \lambda_1}{\partial h} \Big|_{h=0} &= \frac{\partial \lambda_2}{\partial h} \Big|_{h=0} \\ &= \frac{1}{m(1-m^2)} \frac{A_1 C_2 - A_2 C_1}{A_2 \frac{\partial B_1}{\partial \lambda_1} - A_1 \frac{\partial B_2}{\partial \lambda_1}} \\ &\quad \text{for } \alpha = 1, \quad T \leq T_c(1). \end{aligned} \quad (38)$$

The term

$$\left. \frac{\partial \lambda_{1,2}}{\partial h} \right|_{h=0}$$

for the region  $T \geq T_c(\alpha)$  will be given in the next subsection [see Eq. (41)].

#### D. Short-range order parameters and specific heat

Two kinds of short-range order parameters exist in the system considered:  $\tau_x$  which denotes the NN spin correlation which lies along the  $x$ -axis direction and  $\tau_y$  which lies along the  $y$ -axis direction.  $\tau_x$  and  $\tau_y$  are expressed by setting  $\hat{f}_i = \sigma_i$  and  $\hat{f}_i = \sigma_2$  in Eq. (4), respectively, as follows:

$$\tau_x \equiv \langle \sigma_i \sigma_1 \rangle = \langle \sigma_i \hat{K} \rangle + \langle \sigma_i \hat{G} \rangle h, \quad (39a)$$

$$\tau_y \equiv \langle \sigma_i \sigma_2 \rangle = \langle \sigma_2 \hat{K} \rangle + \langle \sigma_2 \hat{G} \rangle h. \quad (39b)$$

In order to evaluate  $\tau_x$  and  $\tau_y$  as functions of temperature with parameter  $\alpha$ , we apply our basic assumption, Eq. (12), to both the rhs's and lhs's of Eqs. (39a) and (39b). We can prove that these resulting two equations again satisfy, for the case of  $h=0$ , the solutions already obtained for  $m$ ,  $\lambda_1$ , and  $\lambda_2$ : Eqs. (28), (26), and (27) below  $T_c(\alpha)$ , and Eqs. (36a) and (36b) above  $T_c(\alpha)$ , respectively.

Finally,  $\tau_x$  and  $\tau_y$  are, for the system without an external field, expressed by

$$\tau_x = m^2 + \lambda_1(1 - m^2), \quad (40a)$$

$$\tau_y = m^2 + \lambda_2(1 - m^2). \quad (40b)$$

At this point let us study the response functions

$$\left. \frac{\partial \lambda_1}{\partial h} \right|_{h=0} \quad \text{and} \quad \left. \frac{\partial \lambda_2}{\partial h} \right|_{h=0}$$

for the region  $T > T_c(\alpha)$ . Since both the correlations  $\langle \sigma_i \hat{G} \rangle$  and  $\langle \sigma_2 \hat{G} \rangle$  are shown to reduce to zero for  $T > T_c(\alpha)$  in the limit  $h \rightarrow 0$ , we obtain, upon differentiating Eqs. (39a) and (39b) with respect to  $h$  and taking  $h \rightarrow 0$ ,

$$\left. \frac{\partial \lambda_1}{\partial h} \right|_{h=0} = \left. \frac{\partial \lambda_2}{\partial h} \right|_{h=0} = 0 \quad \text{for } T > T_c(\alpha). \quad (41)$$

Finally, let us now study the specific heat per site. Since the internal energy per site is defined by  $-J_1 \tau_x - J_2 \tau_y$ , the specific heat per site is given by

$$\begin{aligned} C/k_B &= - \frac{\partial}{\partial (k_B T/J_1)} (\tau_x + \alpha \tau_y) \\ &= - \frac{\partial m^2}{\partial (k_B T/J_1)} [(1 - \lambda_1) + \alpha(1 - \lambda_2)] \\ &\quad - (1 - m^2) \left[ \frac{\partial \lambda_1}{\partial (k_B T/J_1)} + \alpha \frac{\partial \lambda_2}{\partial (k_B T/J_1)} \right]. \quad (42) \end{aligned}$$

In particular, for the region  $T > T_c(\alpha)$ , this reduces to

$$C/k_B = \left[ \frac{J_1}{k_B T} \right]^2 \left[ \operatorname{sech}^2 \left[ \frac{J_1}{k_B T} \right] + \alpha^2 \operatorname{sech}^2 \left[ \frac{\alpha J_1}{k_B T} \right] \right] \quad \text{for } T \geq T_c(\alpha). \quad (43)$$

It should be noted that Eq. (43) becomes exact as  $\alpha \rightarrow 0$ .

We are now in a position to examine the physical properties of anisotropic 2D Ising spin systems numerically. These properties will be given in the next section.

#### IV. NUMERICAL RESULTS AND DISCUSSION

We plot the critical temperature  $T_c(\alpha)$  against the interaction ratio  $\alpha \equiv J_2/J_1$  in Fig. 1 by solving Eq. (29). As obtained in Eq. (30), this yields  $k_B T_c(\alpha=1)/J_1 = 2.885$ , to be compared with  $k_B T_c/J_1^{\text{MFA}} = 4$  and  $k_B T_c/J_1^{\text{series}} = 2.2692$ , and also yields the exact result  $k_B T_c(\alpha=0)/J_1 = 0$ . Thus we understand that Fig. 1 corresponds to an extension of  $T_c$  in the BP method to an anisotropic 2D system. It should also be mentioned that Fig. 1 recovers the result obtained by KT.

The thermal behavior of the CEF's are shown in Fig. 2, through Eqs. (26) and (27) below  $T_c(\alpha)$  and Eqs. (36) above  $T_c(\alpha)$ , for selected values of  $\alpha$ . We observe that both  $\lambda_1$  and  $\lambda_2$  for a fixed ratio  $\alpha$  increase from the value of zero at  $T=0$  K, pass through a maximum value at  $T_c(\alpha)$ , and monotonically decrease with the increase of temperature. But this behavior is changed when the system considered here undergoes, for example, a dilution of magnetic atoms by nonmagnetic atoms;<sup>14</sup> both values of  $\lambda_1$  and  $\lambda_2$  start from a nonzero value at  $T=0$  due to the fact  $m \neq 1$  even at  $T=0$ .

The most important features of  $\lambda_1$  and  $\lambda_2$  are that they show a sharp peak at  $T_c(\alpha)$  due to the phase transition of

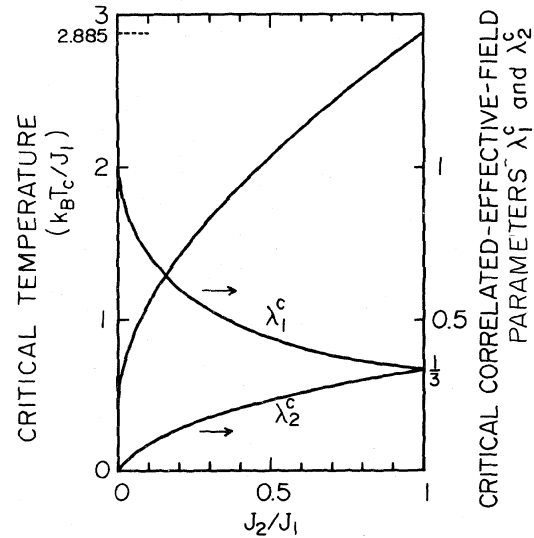


FIG. 1. Critical-temperature curves for anisotropic square-lattice spin- $\frac{1}{2}$  Ising ferromagnet. Two correlated effective-field parameters  $\lambda_1^c = \lambda_1(T_c)$  and  $\lambda_2^c = \lambda_2(T_c)$  at critical temperature are also shown plotted against the ratio  $J_2/J_1$ .

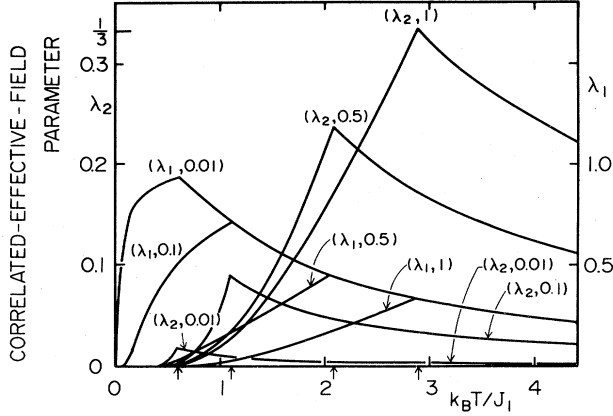


FIG. 2. Thermal behavior of two correlated effective-field parameters  $\lambda_1$  and  $\lambda_2$  for selected values of the ratio  $J_2/J_1$ . The last number in parentheses attached to each curve denotes the values of  $J_2/J_1$ . Note the differences in the scales between  $\lambda_1$  and  $\lambda_2$ .

the system. The magnitude of parameter  $\lambda_1$  ( $\lambda_2$ ) at a critical temperature  $T_c(\alpha)$  increases (decreases) with the decrease of the interaction ratio  $\alpha$ .

The slope of  $\lambda_{1,2}$  for each fixed value of  $\alpha$  plotted against the temperature  $k_B T/J_1$  varies with temperature. The slopes just below critical temperature are particularly important in understanding the thermal behavior of the specific heat, as is seen later. Then, the derivatives

$$\left. \frac{\partial \lambda_1}{\partial (k_B T/J_1)} \right|_{T_c=0} \quad \text{and} \quad \left. \frac{\partial \lambda_2}{\partial (k_B T/J_1)} \right|_{T_c=0}$$

are plotted against  $\alpha$  in Fig. 3. We observe that both

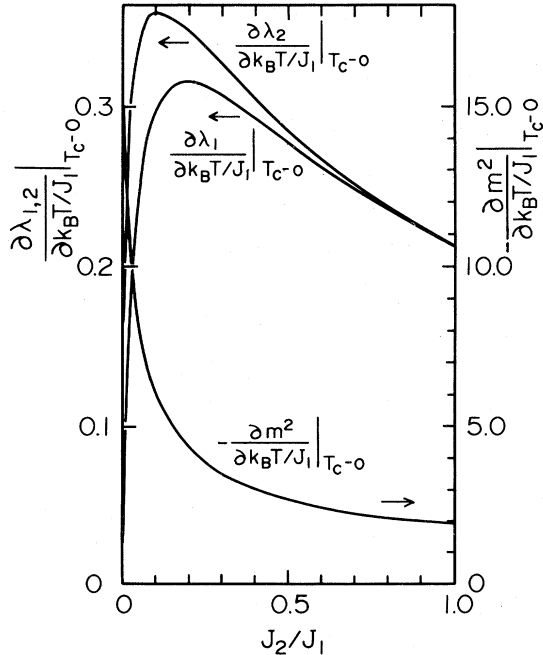


FIG. 3. Three derivatives of  $-m^2$ ,  $\lambda_1$ , and  $\lambda_2$  with respect to  $k_B T/J_1$  just below the critical temperature, plotted against the ratio  $J_2/J_1$ .

derivatives increase from their nonzero value at  $\alpha=1$ , pass through a maximum value at different values of  $\alpha$ , and then decrease rapidly toward zero at  $\alpha=0$  with decreasing  $\alpha$ .

The thermal behavior of the magnetization is given by Eq. (28), from which, as usual in effective-field theories, the classical exponent is derived. The interaction ratio  $\alpha=J_2/J_1$  affects the thermal behavior of the magnetization in such a way that the decrease of  $\alpha$  leads to an increase of the magnetization in the reduced magnetization curve [ $m$ -vs- $T/T_c(\alpha)$  plot] over the entire temperature range for  $T < T_c(\alpha)$ , in comparison with  $\alpha=1$ , that is, the magnetization curve of the isotropic system on the square lattice.

In Fig. 3, in order to understand the thermal behavior of the specific heat, the derivative

$$-\frac{\partial m^2}{\partial (k_B T/J_1)},$$

which measures how rapidly the magnetization falls to zero just below  $T_c(\alpha)$ , is plotted against  $\alpha$ . We observe that the derivative

$$-\frac{\partial m^2}{\partial (k_B T/J_1)}$$

starts at a finite value at  $\alpha=1$ , increases, and finally diverges in the limit  $\alpha \rightarrow 0$  with the decrease of  $\alpha$ .

In Fig. 4, by solving the coupled equations (32), the temperature dependence of the initial inverse susceptibility is shown for selected values of  $\alpha$ . The response functions of  $\lambda_1$  and  $\lambda_2$  in an infinitesimal external field are also shown for selected values of  $\alpha$  in Figs. 5 and 6, respectively.

The system in consideration is essentially two dimensional as long as  $\alpha > 0$ . Accordingly, the initial susceptibility should diverge only once at the critical temperature. This point is clearly illustrated in Fig. 4. Moreover, we observe that (i)  $\chi^{-1} \propto k_B T/J_1$  in the limit  $T \rightarrow \infty$ , (ii) the gradient of  $[J_1/(g\mu_B)^2 \chi]^{-1}$  plotted against  $k_B T/J_1$  just below  $T_c(\alpha)$  is twice of that just above  $T_c$ , (iii) the gra-

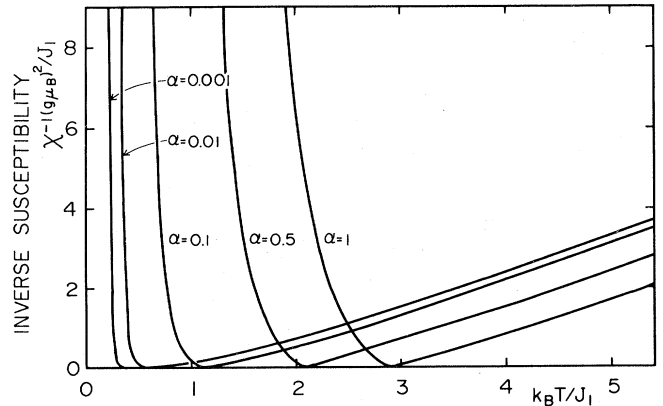


FIG. 4. Temperature dependence of the inverse initial susceptibilities for selected values of the ratio  $\alpha=J_2/J_1$ . On this scale, it is difficult to distinguish among three curves  $\alpha=0$ , 0.01, and 0.001 above  $T_c(\alpha)$ .

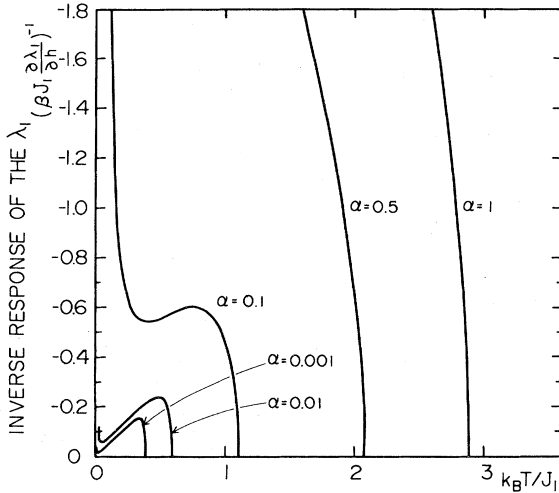


FIG. 5. Curves denoting inverse initial response of  $\lambda_1$  in a magnetic external field plotted against temperature for selected values of the ratio  $\alpha = J_2/J_1$ .

dient slightly below each critical temperature increases with the decrease of  $\alpha$ , and (iv) the inverse susceptibility has an exact, one-dimensional limit [see Eq. (37)]. The inverse susceptibility above  $T_c(\alpha)$  for the system associated with very small  $\alpha$  cannot be distinguished, in Fig. 4, from that of  $\alpha=0$ .

Let us now focus our attention on the response functions

$$\beta J_1 \left. \frac{\partial \lambda_2}{\partial h} \right|_{h=0} \quad \text{and} \quad \beta J_1 \left. \frac{\partial \lambda_1}{\partial h} \right|_{h=0}.$$

From Eq. (32), or Eq. (38) for  $\alpha=1$ , we realize the relation

$$\beta J_1 \left. \frac{\partial \lambda_{1,2}}{\partial h} \right|_{h=0} \propto m^{-1}$$

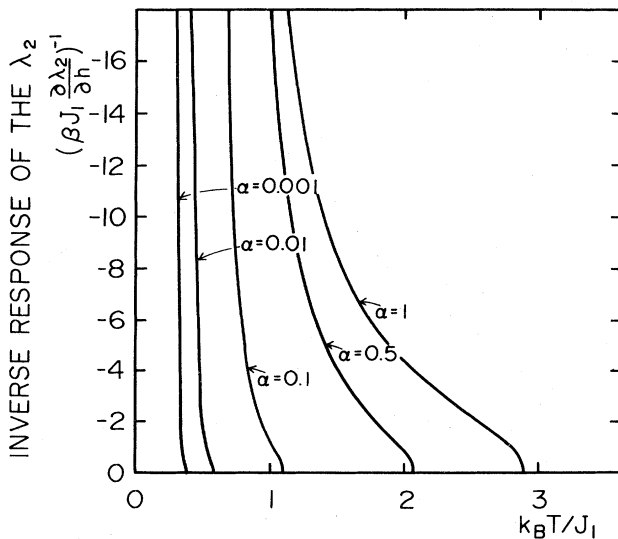


FIG. 6. Curves denoting inverse initial response of  $\lambda_2$  in a magnetic external field plotted against temperature for selected values of the ratio  $\alpha = J_2/J_1$ .

just below  $T_c(\alpha)$ , from which the relation

$$\beta J_1 \left. \frac{\partial \lambda_{1,2}}{\partial h} \right|_{h=0} \propto (1 - T/T_c)^{1/2}$$

is deduced just below  $T_c(\alpha)$ . In fact, this behavior is clearly exhibited in Figs. 5 and 6 for selected values of  $\alpha$ . The characteristic feature is that the sign of the response functions is always negative as long as  $T < T_c(\alpha)$ . This fact may be associated with the resulting decrease of  $\lambda_{1,2}$  when the increase of the  $h$  gives rise to the increase of  $m$ . In particular, the thermal behavior of

$$\left[ \beta J_1 \left. \frac{\partial \lambda_1}{\partial h} \right|_{h=0} \right]^{-1}$$

is anomalous for the case of small  $\alpha$ . This peculiar behavior may be related to the following fact: by decreasing the interaction ratio  $\alpha$ , the parameter  $\lambda_1$  begins to show an upward curvature in the temperature range  $T < T_c(\alpha)$  (see Fig. 2).

On the other hand, the parameters  $\lambda_1$  and  $\lambda_2$  do not respond to vanishingly small  $h$  for the region  $T > T_c(\alpha)$  as shown in Eq. (41). Although  $\lambda_1$  and  $\lambda_2$  sometime behave anomalously in a way that we have pointed out previously, this anomaly is not reflected in the actual physical quantities such as magnetization, susceptibility, short-range order parameter, and specific heat.

In Fig. 7 the temperature dependence of the short-range order parameters, or the NN spin correlation on the  $x$  axis,  $\tau_x$ , and also that on the  $y$  axis,  $\tau_y$ , is depicted for selected values of  $\alpha$  by using Eqs. (40) and (26)–(28) below  $T_c(\alpha)$ , and (40) and (36) above  $T_c(\alpha)$ . These results are qualitatively (and to a certain extent, quantitatively) satisfactory. Finite short-range order parameters continue even above  $T_c(\alpha)$ . The less the value of  $\alpha$ , the more rapidly  $\tau_y$  decreases, around  $T_c(\alpha)$ , to a smaller value. This rapid decrease should be compared with the gradual change of  $\tau_x$ . The most characteristic feature is that the situation  $\tau_x \simeq 1 \gg \tau_y$  near and above  $T_c(\alpha)$  can be realized for small  $\alpha$  or for the quasi-one-dimensional Ising system.

We now turn to the specific heat per site  $C/k_B$ . As  $\alpha \rightarrow 1$ , Eq. (42) gives only the BP result for a simple spa-

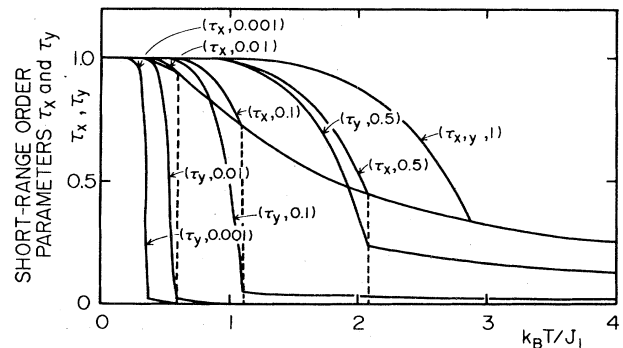


FIG. 7. Thermal behavior of two short-range parameters  $\tau_x$  and  $\tau_y$  for selected values of the ratio  $\alpha = J_2/J_1$ . Numerical figures attached to each curve denote the fixed pair of values  $(\tau_x, \alpha)$  or  $(\tau_y, \alpha)$ . Dashed lines are only to guide the eye to where the critical temperatures are.

tially isotropic 2D system, which we shall discuss further in Sec. V. On the other hand, as  $\alpha \rightarrow 0$ , Eq. (42) gives the exact expression for the 1D isotropic system [see Eq. (43)].

In order to discuss the anisotropic 2D system ( $0 < \alpha < 1$ ), we must remember Fig. 3, in which the derivative at  $T_c(\alpha)$ ,

$$-\left. \frac{\partial m^2}{\partial k_B T / J_1} \right|_{T=T_c(\alpha)},$$

increases with the decrease of the ratio  $\alpha$  and diverges as  $\alpha \rightarrow 0$ . On the other hand, the factor

$$1 - \lambda_1 + \alpha(1 - \lambda_2) = 1 - \tanh(t) + \alpha[1 - \tanh(\alpha t)]$$

at  $T_c(\alpha)$  decreases more rapidly toward zero with the decrease of  $\alpha$ . As a result, the value of the first term on the rhs of Eq. (42), at critical temperature, decreases toward zero with the decrease of  $\alpha$ . The second term on the rhs of Eq. (42) only adds small corrections to the first term. Consequently, the specific heat at  $T_c(\alpha)$  decreases with the decrease of  $\alpha$  and tends to zero as  $\alpha \rightarrow 0$ .

In Fig. 8 the specific-heat curves are shown for selected values of  $\alpha$ . Although the well-known logarithmic singularity is not recovered, an improvement, nevertheless, is obtained in comparison with the MFA results; a paramagnetic tail is present within this formalism. Furthermore, for  $\alpha^* < \alpha < 1$ , the specific heat exhibits a maximum only at critical temperature, and for  $0 < \alpha < \alpha^*$  there exist two maxima, one at critical temperature and one at higher temperature, since in the temperature region  $T > T_c(\alpha)$  the system practically dissociates into the collection of noninteracting chains where  $\alpha^*$  lies between 0.01 and 0.1. Another point is that the peak value at  $T_c(\alpha)$  decreases with the decrease of  $\alpha$ . This satisfying result is derived from the fact that our treatment permits us to distinguish among correlations, for instance,  $\langle \sigma_1 \sigma_3 \rangle$ ,  $\langle \sigma_2 \sigma_4 \rangle$ , and  $\langle \sigma_1 \sigma_2 \rangle$ , in addition to  $\langle \sigma_0 \sigma_1 \rangle$  and  $\langle \sigma_0 \sigma_2 \rangle$ . On the other hand, the MFA and also the effective-field approximation which assumes Eq. (7) (both of which cannot distinguish among these correlations), yields an expression in which any corresponding term to  $(1 - \lambda_1) + \alpha(1 - \lambda_2)$  in Eq. (42) does not exist. As a consequence, this expression gives rise to incorrect behavior,<sup>21</sup> the peak value at  $T_c(\alpha)$  increases with the decrease of  $\alpha$  and diverges in the limit  $\alpha \rightarrow 0$ .

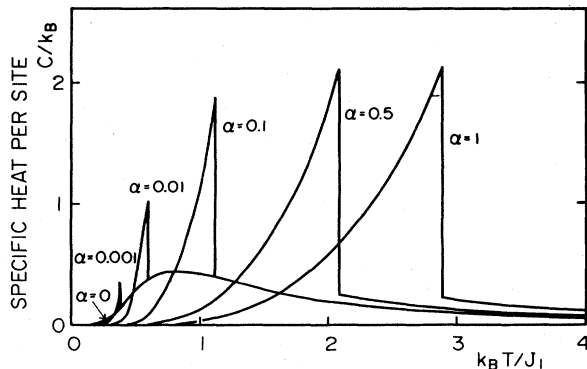


FIG. 8. Temperature dependence of the specific heat per site for selected values of the ratio  $\alpha = J_2 / J_1$ .

We have discussed the anisotropic 2D Ising systems. Within the NCEFT we have calculated the most relevant thermodynamical quantities, such as critical temperature, magnetization, susceptibility, short-range order parameter, and resulting specific heat in analytical forms. We have recovered, in analytical form, all of the results for critical temperature and magnetization obtained by KT, whereas they obtained them only numerically. Interesting features (see Figs. 4 and 8) arise in the thermal behavior of both susceptibility and specific heat due to the fact that the system runs from the 2D to the 1D limit. Here the advantage is the present theory becomes exact as  $\alpha \rightarrow 0$ .

Although CEFP's  $\lambda_1$  and  $\lambda_2$  exhibit some interesting and peculiar behavior, which may be attributed to the fact that these phenomenological parameters are expressed as a composite of the magnetization and the short-range order parameters [see Eqs. (40a) and (40b)], the thermodynamical properties obtained behave normally and are quite satisfactory.

Finally, it is worthwhile to mention the following findings. The present theory starts with three equations, which are derived upon setting, in Eq. (4),  $\bar{f}_i = 1$ ,  $\sigma_1 \sigma_3$ , and  $\sigma_2 \sigma_4$ , i.e., Eqs. (9), (10), and (11), respectively. However, even when we set  $\bar{f}_i = \sigma_1$ ,  $\sigma_2$ ,  $\sigma_1 \sigma_2 \sigma_3$ ,  $\sigma_1 \sigma_2 \sigma_4$ , or  $\sigma_1 \sigma_2 \sigma_3 \sigma_4$ , and introduce the concept of correlated effective fields to these equations [Eqs. (12)], all such equations are proved to satisfy, as solutions for magnetization and the CEFP's, Eqs. (28), (26), and (27) for  $T < T_c(\alpha)$  and  $m = 0$ , and Eq. (36) for  $T > T_c(\alpha)$ . In this way we conclude that the concept of correlated effective fields is consistent with any kind of identity such as Eq. (4), and accordingly has good symmetry. But when the system undergoes disorder,<sup>20</sup> this symmetry may be broken.

## V. THREE-DIMENSIONAL ISING SYSTEM; RELATION BETWEEN THE PRESENT THEORY AND BP THEORY

Let us consider the simple-cubic system with an isotropic NN interaction  $J$  without an external field. Thus the Hamiltonian is given by Eq. (1), where  $J_{ij} = J$  and  $H = 0$ . Our starting point is the Callen identity, into which we introduce the concept of correlated effective-field parameter  $\lambda$  for the sake of evaluating the correlation functions involved in the identity,

$$\sigma_j = \langle \sigma_j \rangle + \lambda(\sigma_i - \langle \sigma_i \rangle), \quad (44)$$

where  $j (= 1, 2, \dots, 6)$  denotes the NN site of a certain central site  $i$ . The parameter  $\lambda$  and the magnetization  $m (= \langle \sigma_i \rangle = \langle \sigma_j \rangle)$  should be determined as a function of temperature to satisfy the following equations:

$$\langle \sigma_i \rangle = \langle \hat{K} \rangle, \quad (45)$$

$$\langle \sigma_i \sigma_j \rangle = \langle \sigma_j \hat{K} \rangle, \quad (46)$$

where

$$\hat{K} = \{ \cosh(D\beta J) + [m + \lambda(\sigma_i - m)] \sinh(D\beta J) \}^6 \tanh x|_{x=0}, \quad (47)$$

and  $j$  denotes one of the NN sites of  $i$ .



These coupled equations are solved as follows:

$$m = \tanh \left[ \frac{Z}{Z-1} L^* \right] = \frac{e^{2t} \sinh(2L^*)}{e^{2t} \cosh(2L^*) + 1}, \quad (48)$$

$$\tau = 1 - \frac{2}{e^{2t} \cosh(2L^*) + 1}, \quad (49)$$

$$\lambda = \frac{\tau - m^2}{1 - m^2}, \quad (50)$$

where  $Z$  denotes the coordination number (now  $Z=6$ ), and  $\tau$  denotes the NN correlation function  $\langle \sigma_i \sigma_j \rangle$ ,  $t \equiv J/k_B T$ , and  $L^*$  is given by the following equations:

$$\cosh(2L^*) = \frac{1}{4} \{ e^{10t} - 5e^{2t} + [(e^{10t} - 5e^{2t})^2 + 4(5e^{8t} - 10e^{4t} + 1)]^{1/2} \} \quad \text{for } T \leq T_c, \quad (51a)$$

$$L^* = 0 \quad \text{for } T \geq T_c, \quad (51b)$$

where

$$k_B T_c / J = 2(\ln 1.5)^{-1} = 4.9326.$$

At this point it is worthwhile to discuss the  $L^*$ . Then we shall consider the Ising system with a NN exchange interaction without an external field on any lattice with a coordination number  $Z$ . In the so-called BP theory, the Hamiltonian considered Eq. (1) for the case of  $H=0$  is replaced by the  $Z+1$  body-truncated cluster Hamiltonian,

$$-\beta \mathcal{H}_{\text{BP}} = \beta \sum_j J_{ij} \sigma_i \sigma_j + \tilde{L}^* \sum_j \sigma_j, \quad (52)$$

where  $\tilde{L}^*$  represents the effective fields due to  $Z-1$  NN spins outside of the cluster. We find that the  $L^*$  which appeared in Eqs. (48) and (49) does completely coincide with  $\tilde{L}^*$  defined above. Furthermore, Eqs. (48)–(50) are valid for any coordination number, provided that

$$L^* = 0 \quad \text{for } Z = 2, \quad (53)$$

$$\cosh(2L^*) = \begin{cases} \frac{1}{2}(e^{4t} - 2e^{2t} - 1) & \text{for } Z = 3, T \leq T_c, \\ 1 & \text{for } Z = 3, T > T_c, \end{cases} \quad (54)$$

and

$$\cosh(2L^*) = \begin{cases} \frac{1}{2}(e^{6t} - 3e^{2t}) & \text{for } Z = 4, T \leq T_c, \\ 1 & \text{for } Z = 3, T > T_c, \end{cases} \quad (55)$$

where

$$k_B T_c / J = 2 / \ln[Z / (Z - 2)]. \quad (56)$$

For any  $Z$  and in the region of  $T \geq T_c$ , Eq. (49) reduces to  $\tau = \tanh(J/k_B T)$  because of  $L^* = 0$ . In this way, we conclude that the NCEFT gives the same thermodynamical quantities for the Ising model with isotropic NN exchange interactions on a regular lattice as does BP theory. It is quite interesting to note that, although the philoso-

phy on which these two theories is based is different from each other, they predict the same physical properties.

## VI. CONCLUSIONS

We have discussed the spin- $\frac{1}{2}$  Ising ferromagnet in an anisotropic square lattice. Within a new type of correlated effective-field theory we calculated the theory's correlated effective-field parameters, including its response in a vanishingly small magnetic external field and the most relevant thermodynamical quantities, namely the critical temperature, magnetization, susceptibility, and specific heat.

The correlated effective-field parameters  $\lambda_1$  and  $\lambda_2$  exhibit interesting behavior with the change of the exchange ratio  $\alpha = J_2/J_1$ . The CEF's response in the infinitesimal external magnetic field

$$\beta J_1 \left. \frac{\partial \lambda_{1,2}}{\partial h} \right|_{h=0}$$

is negative and proportional to

$$\left[ 1 - \frac{T}{T_c(\alpha)} \right]^{-1/2}$$

just below the critical temperature  $T_c(\alpha)$ ; on the other hand, it is zero above  $T_c(\alpha)$ . In particular, the  $\lambda_1$  and

$$\beta J_1 \left. \frac{\partial \lambda_1}{\partial h} \right|_{h=0}$$

behave anomalously for small  $\alpha$  ( $\alpha < 0.1$ ). These results may be attributed to the fact that the  $\lambda_1$  and  $\lambda_2$  measure, as a result, the NN correlation function itself above  $T_c(\alpha)$ ; however, the CEF's  $\lambda_1$  and  $\lambda_2$  measure, as a result, a composite of the NN correlation function and magnetization below  $T_c(\alpha)$ .

Interesting effects (see Figs. 4 and 8) arise in the thermal behavior of both susceptibility and specific heat with the change of interaction ratio  $\alpha=1$  (pure 2D)  $\rightarrow$  0 (pure 1D); inverse susceptibility becomes zero only at  $T_c(\alpha)$  and its slope against a temperature slightly below each  $T_c(\alpha)$  increases with the decrease of  $\alpha$ . The value of the specific heat at  $T_c(\alpha)$  decreases with the decrease of  $\alpha$ . In particular, for moderately small  $\alpha$  the specific heat exhibits one peak due to the phase transition and a broad maximum due to the near separation of the system into noninteracting chains. Thus the crossover from 2D to 1D is clearly exhibited even in the level of the so-called MFA.

We have verified that the NCEFT reproduces all of the thermodynamical quantities derived by the BP method for the spin- $\frac{1}{2}$  Ising ferromagnet on a  $Z$ -coordinated regular lattice. It should be pointed out that our theory is completely different in its formulation from the BP method and has an advantage in its conceptual and mathematical simplicity.

The formalism of the EFA [see Eq. (7)] has been applied to bond random magnets,<sup>18</sup> amorphous systems,<sup>18</sup>

binary alloys,<sup>18</sup> spin-glasses,<sup>18</sup> the transverse Ising model,<sup>18</sup> and the Potts model.<sup>22</sup> Consequently, the methods developed in this paper should be able to be applied to these systems as well as more complex systems. Moreover, the correlation identities are not restricted to the spin- $\frac{1}{2}$  Ising model. As a result, the NCEFT may be suitable even for analyzing these systems.

## ACKNOWLEDGMENTS

The author would like to thank Dr. T. Kaneyoshi for a critical reading of manuscript and valuable comments, and also thanks Dr. E. F. Sarmiento for several helpful comments. This work was partially supported by Conselho Nacional de Desenvolvimento Científico e Tecnológico (Brazil).

## APPENDIX

$$K_1 \equiv \cosh^2(Dt\alpha)\cosh(Dt)\sinh(Dt)\tanh x \Big|_{x=0} \\ = \frac{1}{8} \{ \tanh[2t(1+\alpha)] + \tanh[2t(1-\alpha)] + 2 \tanh(2t) \} , \quad (\text{A1})$$

$$K_2 \equiv \cosh^2(Dt)\cosh(Dt\alpha)\sinh(Dt\alpha)\tanh x \Big|_{x=0} \\ = \frac{1}{8} \{ \tanh[2t(1+\alpha)] - \tanh[2t(1-\alpha)] + 2 \tanh(2t\alpha) \} , \quad (\text{A2})$$

$$K_3 \equiv \cosh(Dt\alpha)\sinh[Dt(1+\alpha)]\sinh^2(Dt)\tanh x \Big|_{x=0} \\ = \frac{1}{8} \{ \tanh[2t(1+\alpha)] - \tanh[2t(1-\alpha)] - 2 \tanh(2t\alpha) \} , \quad (\text{A3})$$

$$K_4 \equiv \cosh(Dt)\sinh(Dt)\sinh^2(Dt\alpha)\tanh x \Big|_{x=0} \\ = \frac{1}{8} \{ \tanh[2t(1+\alpha)] + \tanh[2t(1-\alpha)] - 2 \tanh(2t) \} , \quad (\text{A4})$$

$$G_1 \equiv \cosh^2(Dt)\cosh^2(Dt\alpha)\text{sech}^2 x \Big|_{x=0} \\ = \frac{1}{8} \{ \text{sech}^2[2t(1+\alpha)] + \text{sech}^2[2t(1-\alpha)] + 2 \text{sech}^2(2t) + 2 \text{sech}^2(2t\alpha) + 2 \} , \quad (\text{A5})$$

$$G_2 \equiv \cosh(Dt)\sinh(Dt)\cosh(Dt\alpha)\sinh(Dt\alpha)\text{sech}^2 x \Big|_{x=0} \\ = \frac{1}{8} \{ \text{sech}^2[2t(1+\alpha)] - \text{sech}^2[2t(1-\alpha)] \} , \quad (\text{A6})$$

$$G_3 \equiv \cosh^2(Dt\alpha)\text{sech}^2(Dt)\text{sech}^2 x \Big|_{x=0} \\ = \frac{1}{8} \{ \text{sech}^2[2t(1+\alpha)] + \text{sech}^2[2t(1-\alpha)] + 2 \text{sech}^2(2t) - 2 \text{sech}^2(2t\alpha) - 2 \} , \quad (\text{A7})$$

$$G_4 \equiv \sinh^2(Dt\alpha)\cosh^2(Dt)\text{sech}^2 x \Big|_{x=0} \\ = \frac{1}{8} \{ \text{sech}^2[2t(1+\alpha)] + \text{sech}^2[2t(1-\alpha)] - 2 \text{sech}^2(2t) + 2 \text{sech}^2(2t\alpha) - 2 \} , \quad (\text{A8})$$

$$G_5 \equiv \sinh^2(Dt)\sinh^2(Dt\alpha)\text{sech}^2 x \Big|_{x=0} \\ = \frac{1}{8} \{ \text{sech}^2[2t(1+\alpha)] + \text{sech}^2[2t(1-\alpha)] - 2 \text{sech}^2(2t) - 2 \text{sech}^2(2t\alpha) + 2 \} . \quad (\text{A9})$$

<sup>1</sup>L. Onsager, Phys. Rev. **65**, 117 (1944); C. N. Yang, *ibid.* **85**, 808 (1952).

<sup>2</sup>M. F. Sykes, D. S. Gaunt, P. D. Roberts, and J. A. Wyley, J. Phys. A **5**, 640 (1972).

<sup>3</sup>Th. Niemeijer and J. M. J. van Leeuwen, in *Phase Transitions and Critical Phenomena*, edited by C. Domb and M. S. Green (Academic, London, 1976), Vol. 6.

<sup>4</sup>H. A. Bethe, Proc. R. Soc. London, Ser. A **150**, 552 (1935); R. Peierls, Proc. Cambridge Philos. Soc. B **2**, 477 (1936); Y. Takagi, J. Phys. Soc. Jpn. **4**, 99 (1949); R. H. Fowler and E. A. Guggenheim, Proc. R. Soc. London, Ser. A **174**, 189 (1940).

<sup>5</sup>M. E. Lines, Phys. Rev. B **9**, 3927 (1974).

<sup>6</sup>N. Suzuki, T. Isu, and K. Motizuki, Solid State Commun. **23**, 319 (1977).

<sup>7</sup>W. A. Gusmão and C. Scherer, Phys. Status Solidi B **92**, 595 (1979).

<sup>8</sup>P. B. Fynbo, Physica **105A**, 517 (1981).

<sup>9</sup>T. Kaneyoshi, I. P. Fittipaldi, R. Honmura, and T. Manabe,

Phys. Rev. B **24**, 481 (1981).

<sup>10</sup>H. B. Callen, Phys. Lett. **4**, 161 (1963).

<sup>11</sup>R. Honmura and T. Kaneyoshi, Prog. Theor. Phys. (Kyoto) **60**, 635 (1978); J. Phys. C **12**, 3979 (1979).

<sup>12</sup>T. Kaneyoshi and I. Tamura, Phys. Rev. B **25**, 4679 (1982).

<sup>13</sup>G. B. Taggart, Physica **116A**, 34 (1982).

<sup>14</sup>T. Kaneyoshi, I. Tamura, and R. Honmura, Phys. Rev. B **29**, 2769 (1984).

<sup>15</sup>I. Tamura, E. F. Sarmiento, I. P. Fittipaldi, and T. Kaneyoshi, Phys. Status Solidi B **118**, 409 (1983).

<sup>16</sup>M. E. Fisher, Phys. Rev. **113**, 969 (1959); R. A. Tahir-Kheli, B. G. S. Doman, and D. ter Haar, Phys. Lett. **4**, 5 (1963); M. Suzuki, *ibid.* **19**, 267 (1965).

<sup>17</sup>H. Mamada and F. Takano, J. Phys. Soc. Jpn. **25**, 675 (1968); N. Matsudaira, J. Phys. Soc. Jpn. **35**, 1593 (1973); T. Kaneyoshi, Phys. Lett. **76A**, 67 (1980); A. R. Ferchmin, IEEE Trans. Magn. **MAG-18**, 7/4 (1982).

<sup>18</sup>For bond random magnets, see T. Kaneyoshi, I. P. Fittipaldi,

and H. B. Beyer, *Phys. Status Solidi B* **102**, 393 (1980); E. F. Sarmiento and C. Tsallis, *Phys. Rev. B* **27**, 5784 (1983); R. Honmura, E. F. Sarmiento, and C. Tsallis, *Z. Phys. B* **51**, 355 (1983). For amorphous systems, see T. Kaneyoshi and H. Beyer, *J. Phys. Soc. Jpn.* **49**, 1306 (1980); T. Kaneyoshi and I. P. Fittipaldi, *Phys. Status Solidi B* **105**, 629 (1981); R. Honmura, I. P. Fittipaldi, E. F. Sarmiento, and T. Kaneyoshi, *J. Magn. Magn. Mater.* **31-34**, 1485 (1983). For binary alloys, see R. Honmura, A. F. Khater, I. P. Fittipaldi, and T. Kaneyoshi, *Solid State Commun.* **41**, 385 (1982). For spin-

glasses, see T. Kaneyoshi, *Phys. Rev. B* **24**, 2693 (1981). For the transverse Ising model, see F. C. Sá Barreto, I. P. Fittipaldi, and B. Zeks, *Ferroelectrics* **39**, 1103 (1981).

<sup>19</sup>F. Zernike, *Physica* **7**, 565 (1940).

<sup>20</sup>G. B. Taggart and I. P. Fittipaldi, *Phys. Rev. B* **25**, 7026 (1982). See also G. B. Taggart, *Physica* **113A**, 535 (1982).

<sup>21</sup>E. F. Sarmiento, R. Honmura, and C. Tsallis, *Rev. Bras. Fís.* **13**, 303 (1983).

<sup>22</sup>R. Honmura, E. F. Sarmiento, C. Tsallis, and I. P. Fittipaldi, *Phys. Rev. B* **29**, 2761 (1984).